Journal of Hazardous Materials 219–220 (2012) 111–118

Contents lists available at SciVerse ScienceDirect

Journal of Hazardous Materials

journal homepage: www.elsevier.com/locate/jhazmat

Root uptake and phytotoxicity of nanosized molybdenum octahedral clusters

Tangi Aubert[a], Agnès Burel[b], Marie-Andrée Esnault[c], Stéphane Cordier[a], Fabien Grasset[a], Francisco Cabello-Hurtado[c,*]

[a] Solid State Chemistry and Materials Group, UMR CNRS 6226 Sciences Chimiques de Rennes, University of Rennes 1, 263 av. du Général Leclerc, Campus de Beaulieu, 35042 Rennes, France
[b] Electronic Microscopy Department, University of Rennes 1, 2 av. du Professeur Léon-Bernard, Campus de Villejean, 35043 Rennes, France
[c] Mechanisms at the Origin of Biodiversity Team, UMR CNRS 6553 Ecobio, University of Rennes 1, 263 av. du Général Leclerc, Campus de Beaulieu, 35042 Rennes, France

ARTICLE INFO

Article history:
Received 18 January 2012
Received in revised form 20 March 2012
Accepted 22 March 2012
Available online 29 March 2012

Keywords:
Nanomaterials
Nanotoxicity
Metal atom clusters
Rapeseed
NanoSIMS

ABSTRACT

Here are examined the root uptake and phytotoxicity of octahedral hexamolybdenum clusters on rapeseed plants using the solid state compound $Cs_2Mo_6Br_{14}$ as cluster precursor. $[Mo_6Br_{14}]^{2-}$ cluster units are nanosized entities offering a strong and stable emission in the near-infrared region with numerous applications in biotechnology. To investigate cluster toxicity on rapeseed plants, two different culture systems have been set up, using either a water-sorbing suspension of cluster aggregates or an ethanol-sorbing solution of dispersed nanosized clusters. Size, shape, surface area and state of clusters in both medium were analyzed by FE-SEM, BET and XPS. The potential contribution of cluster dissolution to phytotoxicity was evaluated by ICP-OES and toxicity analysis of Mo, Br and Cs. We showed that the clusters did not affect seed germination but greatly inhibited plant growth. This inhibition was much more important when plants were treated with nanosized entities than with microsized cluster aggregates. In addition, nanosized clusters affected the root morphology in a different manner than microsized cluster aggregates, as shown by FE-SEM observations. The root penetration of the clusters was followed by secondary ion mass spectroscopy with high spatial resolution (NanoSIMS) and was also found to be much more important for treatments with nanosized clusters.

1. Introduction

Nanosciences reveal a great potential of development for all disciplines and types of applications [1,2]. The physicochemical properties of materials at the scale of nanoparticles (diameter < 100 nm) can greatly differ from those of the corresponding bulk materials [3]. The size reduction of matter allows nanomaterials to execute novel activities such as luminescence, plasmon resonance, catalysis, magnetism, etc., but can also bring new toxic effects which were not known so far [4]. Among the characteristics of nanomaterials, those suspected to be responsible for nanotoxic effects are commonly: the size, the shape, the high specific surface area, the appearing reactivity of formerly inert materials, the possibility of crossing natural barriers, the solubility, the stability in liquid medium or in the air, etc. [1,4]. All these new parameters have now to be carefully considered in toxicological studies.

Among nanomaterials, nanosized systems with luminescence properties have tremendous potential applications in biotechnology and information technology such as biological imaging, sensors, microarrays and optical computing. However, the design of non toxic and robust luminescent systems emitting in the near-infrared region is still an open challenge for nanobiotechnologies [5]. In this frame, new systems incorporating luminescent $[Mo_6X_{14}]^{2-}$ cluster units (X = Cl, Br, or I) inside monodispersed and size-controlled silica nanoparticles have been recently developed in our group [6–8]. Besides, molybdenum hexanuclear clusters are already involved in several patents for applications in biotechnology as contrast agents [9], oxygen sensors [10] and in display technologies [11]. A responsible development of nanotechnologies should imply toxicity studies of each new nanomaterial. If those molybdenum clusters are meant to be commercialized, their toxicity, as part of the required risk evaluation, should be perfectly known.

Most of the work performed on the toxicology of nanoparticles dealt with animal/human health and safety, whereas environmental health has been often neglected [1,4,12]. Plants, as important environmental components and sinks in terrestrial and aquatic ecosystems, are essential living organisms for testing ecological effects of nanoparticles [13]. Thus, the study of the potential uptake and accumulation of nanoparticles by plants and their subsequent fate within food chains are of great importance. Despite this, research on nanotoxicity using plants is still scarce. Most of the available studies on nanoparticles phytotoxicity reported negative

* Corresponding author. Tel.: +33 223235022; fax: +33 223235026.
E-mail address: francisco.cabello@univ-rennes1.fr (F. Cabello-Hurtado).

0304-3894/$ – see front matter © 2012 Elsevier B.V. All rights reserved.
http://dx.doi.org/10.1016/j.jhazmat.2012.03.058

effects of some nanoparticles on higher plants [14]. The uptake and bioaccumulation of nanoparticles by plants is crucial, and several studies have shown that some nanoparticles can enter plant cells [14,15] despite the limited size (around 4 nm) of pores in plant cell walls [16]. However, the mechanisms of penetration of nanoparticles in plants are not clearly understood yet. Rico et al. recently made a review on the proposed pathways found in the current literature [17].

The present study is intended for obtaining data on the acute environmental toxicity of nanosized molybdenum clusters. In this frame, the ternary halide $Cs_2Mo_6Br_{14}$ (CMB) was used as precursor of $[Mo_6Br_{14}]^{2-}$ cluster units for investigating the effects of these nanosized entities on seed germination and seedling growth, as well as their possible penetration and accumulation on rapeseed (*Brassica napus*), a commercially important plant. In addition, these clusters proved to be an interesting system since they aggregate or remain nanosized depending on the dispersing medium. It was therefore interesting to study their effect on plants for fundamental aspects of nanotoxicity studies. Thus, the present study is focusing on how the size and shape of the material conditioned its toxic effects and penetration into rapeseed plants.

2. Materials and methods

2.1. $Cs_2Mo_6Br_{14}$ cluster precursor

$Cs_2Mo_6Br_{14}$ was used as the precursor of $[Mo_6Br_{14}]^{2-}$ cluster units (see Supplementary data). This precursor is prepared by solid state chemistry at high temperature as described in the literature [18] and can be dispersed as nanosized entities (1 nm) in ethanolic solution [6].

2.2. Plant culture systems and biomass determination

Seeds of rapeseed (*B. napus*) of the drakkar ecotype have been used. Plant culture system and test procedures have been adapted from U.S. EPA guidelines [13]. The cultures were performed on sterilized filter papers (Whatman no. 3) disposed in 90 mm × 15 mm Petri dishes that contain 4 ml of the appropriate culture medium (described below). The dishes, containing 8 seeds each, were sealed and placed in a phytotron for germination and growth of the plants at 24 °C in the dark. After 5 days of growth, the seedlings were collected. The fresh shoots and roots were separated and their biomass was immediately measured. Each experiment was conducted three times, i.e. three Petri dishes containing eight seedlings each. The biomass results are presented as mean ± SE (standard error of the mean) of the three independent experiments. Differences between means were evaluated for significance by one-way analysis of variance (ANOVA) and Duncan's test for multiple comparisons, and by Student's *t*-test for pairwise comparisons. Statistical significance was accepted when $p < 0.05$.

Two procedures have been used to introduce the clusters into the culture substrate. In the first system, denoted as H_2O-CMB, the clusters were directly dispersed in Milli-Q water and 4 ml of the resulting suspension were placed in the Petri dish. In the second system, denoted as EtOH-CMB, the clusters were solubilized in a 95% ethanol solution and 4 ml of this solution were placed in the Petri dish. In order to avoid solvent toxicity, the ethanol was completely removed by evaporation in a laminar fume for 24 h, and 4 ml of Milli-Q water were added to the Petri dish. Corresponding controls have been prepared by dispersing either pure water or ethanol in Petri dishes, and following a similar procedure as above. The pH of the culture medium with and without plant growth was measured. In addition, to estimate the toxicological potential of dissolved elements compared to the clusters themselves, we treated plants with either CsBr, KBr or K_2MoO_4 water solutions.

2.3. Culture medium characterizations

The modifications experienced by the cluster compound in the culture medium have been characterized from different points of view. The size and morphology of the cluster aggregates have been characterized by direct observation of the dried culture substrates (filter paper) using field emission scanning electron microscopy (FE-SEM). The specific surface area of the cluster aggregates in the H_2O-CMB system was determined by the Brunauer–Emmett–Teller method (BET) using a Micromeritics Tristar 3000. This specific surface area was measured on a powder of aggregates obtained by centrifugation of a 1 mM suspension of $Cs_2Mo_6Br_{14}$ in water and dried in room conditions. The exact state of the clusters was determined by X-ray photoemission spectroscopy (XPS) measurements, directly on the dried culture substrates for both H_2O-CMB and EtOH-CMB systems at 1 mM, and on the starting $Cs_2Mo_6Br_{14}$ powder.

To estimate the possible dissolution of the clusters, the medium of culture systems, with and without seeds, were collected after 5 days and centrifuged (RCF = 25,000 × *g*, 30 min) to eliminate all the possible solid elements. Mo and Br were dosed on the centrifuge clarified liquid parts by inductively coupled plasma optical emission spectrometry (ICP-OES).

2.4. NanoSIMS analysis

The presence of the clusters inside the roots was analyzed by secondary ion mass spectrometry with high spatial resolution (NanoSIMS). A 16-keV cesium primary ionic source was focused with a spatial resolution of ~120 nm and raster-scanned on the sample surface for the mapping of negative secondary ions ($^{12}C^{14}N^-$ and $^{81}Br^-$). Later, on the same samples, a 16-keV oxygen primary ionic source was focused with a spatial resolution of ~400 nm and raster-scanned on the sample surface for the mapping of positive secondary ions ($^{98}Mo^+$).

3. Results

3.1. Characterization of the clusters in the culture systems

It is worth noting that the solubilization of $Cs_2Mo_6Br_{14}$ in a 95% ethanol solution leads to a stable dispersion of nanosized $[Mo_6Br_{14}]^{2-}$ cluster units, and the EtOH-CMB sorbing medium can be considered as a true solution [6]. On the other hand, even if $Cs_2Mo_6Br_{14}$ is firstly soluble in water, it reacts instantly and exchanges its apical Br ligands for OH groups or water molecules [19], according to the following hydrolysis reaction:

$$Cs_2Mo_6Br_{14} + xH_2O \rightarrow [(Mo_6Br^i_8)(OH)^a_4(H_2O)^a_2]\cdot 12H_2O + 2Cs^+ + 6Br^- + 4H_3O^+$$

The resulting $[(Mo_6Br^i_8)(OH)^a_4(H_2O)^a_2]\cdot 12H_2O$ cluster-based compound is not soluble in water and precipitates, forming microsized aggregates that sediment rapidly. Hence, the H_2O-CMB sorbing medium is a suspension.

The state of the clusters in both culture systems has been characterized by FE-SEM observations of the inert substrates (Fig. 1). The clusters in the H_2O-CMB system form disc-like aggregates which are of few micrometers in size (mean size = 2.3 ± 0.5 μm in diameter and 390 ± 60 nm in thickness). On the other hand, the clusters in the EtOH-CMB system also show disc-like or rod-like aggregates but they are bellow the micrometer range (mean size = 550 ± 180 nm in diameter and 100 ± 30 nm in thickness). Thus, the two

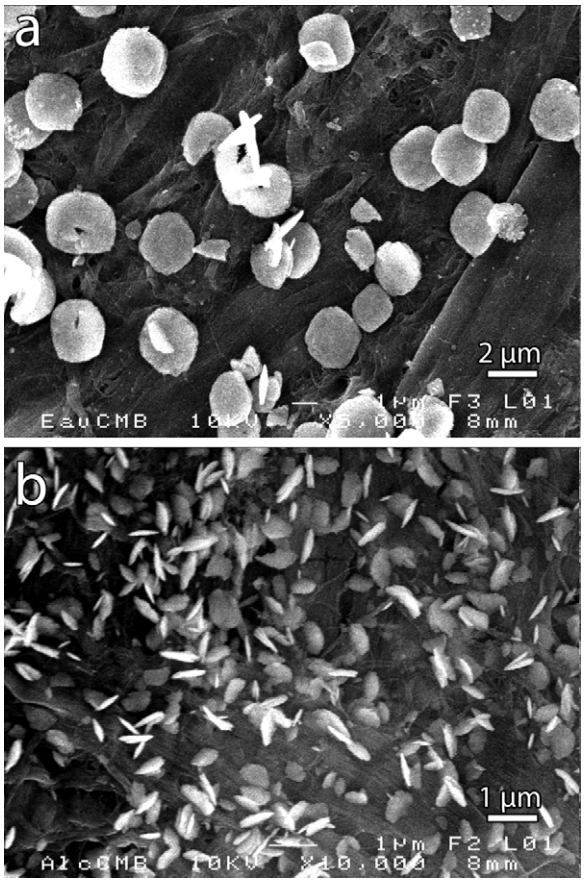

Fig. 1. FE-SEM images of the culture substrates for (a) H_2O-CMB and (b) EtOH-CMB systems.

different culture systems allowed studying the effects of clusters in two different forms.

The aggregation of the clusters observed in both systems may have an influence on their specific surface area which is an important parameter to consider in toxicological studies. It is not possible to collect the cluster aggregates from the culture medium without affecting their morphology. However, for H_2O-CMB system the aggregates are formed directly in water and before being spread on the substrate. Thus, the cluster aggregates gathered by centrifugation of a H_2O-CMB suspension are similar to those in the culture medium. For this system, the cluster aggregates showed to have a specific surface area of $7.3 \pm 0.2\ m^2/g$. In the EtOH-CMB system, it is not possible to simulate the aggregation process outside of the culture medium because the formation of these aggregates occurs when isolated clusters are in interaction with the substrate. In addition, the FE-SEM images showed that for the EtOH-CMB system, the cluster aggregates are partially buried in the filter paper (Fig. 1b). Thus, we have no information on the state of the clusters under the surface. They can be adsorbed in the fibers of the filter paper without being aggregated due to an interaction with this substrate and remain as truly nanosized. If we consider a $[Mo_6Br_{14}]^{2-}$ cluster unit and its Cs^+ counter cations as inscribed in a perfectly smooth sphere with a diameter of 1 nm, the theoretical specific surface area would be about $1000\ m^2/g$. Thus, the cluster species in the EtOH-CMB system may have a specific surface area which can range between 7 and $1000\ m^2/g$, with a wide distribution within the system as confirmed below.

As shown by the hydrolysis reaction given above, the hydrolysis of the cluster compound should result in a pH decrease. Indeed, the pH measurements performed on mediums prepared in the conditions of culture, but without receiving seeds, showed a pH decrease proportional with the cluster concentration (Supplementary information Fig. S2). In addition, the pH was found equivalent for both systems at a given cluster concentration, indicating that the hydrolysis rate might be similar in both systems. However, in the presence of seedlings the pH of mediums always appeared to be neutral, regardless the cluster concentration. Somehow, the plants were able to neutralize the acidic pH.

The Mo and Br elements have been dosed by ICP-OES in the "centrifuge clarified" liquid parts of culture mediums treated with 1 mM of clusters. In the H_2O-CMB system without plant growth, the analyses showed an average Br concentration of 4.91 ± 0.01 mM, but no trace of Mo. This Br concentration indicates that 82% of the apical Br ligands (i.e. roughly 5 Br ligands over the 6 initially bonded to the cluster) were released in solution due to the hydrolysis of the clusters. In the H_2O-CMB system with plant growth, there were still no Mo, but the average Br concentration was 4.43 ± 0.04 mM. This finding demonstrates that the presence of plants diminished the Br concentration in the medium. In the EtOH-CMB system without plant growth, the average Mo and Br concentrations were 1.26 ± 0.03 mM and 6.12 ± 0.07 mM respectively. However, these solutions appeared as perfectly transparent with an intense yellow coloration, and their UV absorption spectra showed the typical signature of cluster units (Supplementary information Fig. S3). Thus, we can assume that the Mo found in solution does not correspond to ionic species resulting from the dissolution of clusters, but from truly non-aggregated and nanosized cluster units that could not be removed from the supernatants by centrifugation. The Mo concentration indicates that 21% of the cluster units remained as truly nanosized and dispersed in the liquid part of the culture medium. This is in agreement with the hypothesis for the estimation of the specific surface area of the clusters in the EtOH-CMB system. The high Br concentration hence comes from the Br associated with the clusters and from the apical Br ligands of the hydrolyzed clusters. In the EtOH-CMB system with plant growth, the average Mo and Br concentrations were 0.22 ± 0.14 mM and 4.63 ± 0.20 mM respectively. Thus, the presence of plants diminished the concentration of cluster units in the medium.

The hydrolysis of the clusters and the release of apical Br ligands when reacting with water have also been characterized with XPS measurements (Supplementary information Fig. S4). The obtained spectra clearly showed a diminution in the intensities of the Br^a peaks in both culture systems compared to the starting $Cs_2Mo_6Br_{14}$ powder. The diminution of the Br^a peaks is equivalent in H_2O-CMB and EtOH-CMB systems, confirming the equivalent hydrolysis rate. In addition, if some clusters were completely decomposed in the culture medium, it would have been visible from XPS analysis through the apparition of a new peak at 235 eV corresponding to the oxidation of the Mo (from oxidation number II to VI) and formation of MoO_3. Such result has never been observed by XPS analysis on the culture substrates (data not shown).

3.2. *Effects of $Cs_2Mo_6Br_{14}$ on rapeseed growth and development*

A concentration of 1 mM has firstly been adopted to investigate the phytotoxicity of $Cs_2Mo_6Br_{14}$. Nearly 100% of the control seeds had germinated after 5 days in the dark. The experiments showed that seed germination was never affected by the clusters. In contrast, all the $Cs_2Mo_6Br_{14}$ treatments at 1 mM provoked a substantial inhibition of the roots and shoots growth as seen from the biomass results (Fig. 2), the roots being always more affected than the shoots ($p_{H_2O\text{-CMB}} = 0.00001$, $p_{EtOH\text{-CMB}} = 0.0001$). In addition, the inhibition was significantly higher in EtOH-CMB than in H_2O-CMB ($p_{roots} = 0.00001$, $p_{shoots} = 0.0029$).

In addition, to estimate the toxicological potential of dissolved elements compared to the clusters themselves, we treated

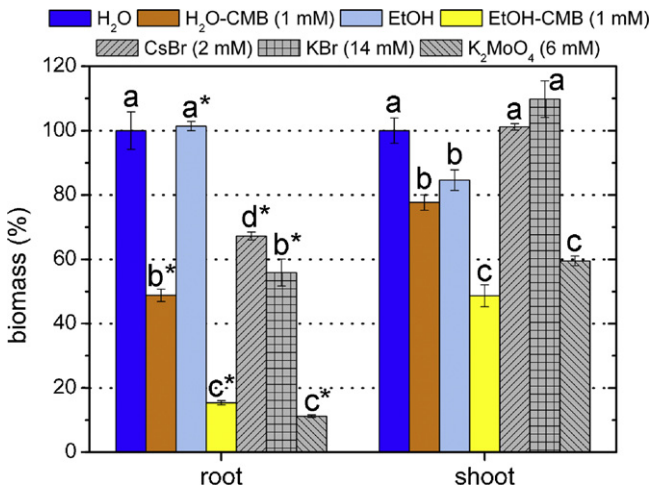

Fig. 2. Biomass results for the water-sorbing suspension (H_2O-CMB) and the ethanol-sorbing solution (EtOH-CMB) at 1 mM, compared with the negative controls (H_2O and EtOH) and with CsBr (2 mM), KBr (14 mM) and K_2MoO_4 (6 mM) solutions. All the root and shoot growth data are respectively expressed as percentages of the root or shoot growth in H_2O negative control. Significant differences among root or shoot biomass values are marked with different letters ($p < 0.05$). Significant differences between effects of a treatment on shoots and roots are marked with an asterisk ($p < 0.05$). (For interpretation of the references to color in this artwork, the reader is referred to the web version of the article.)

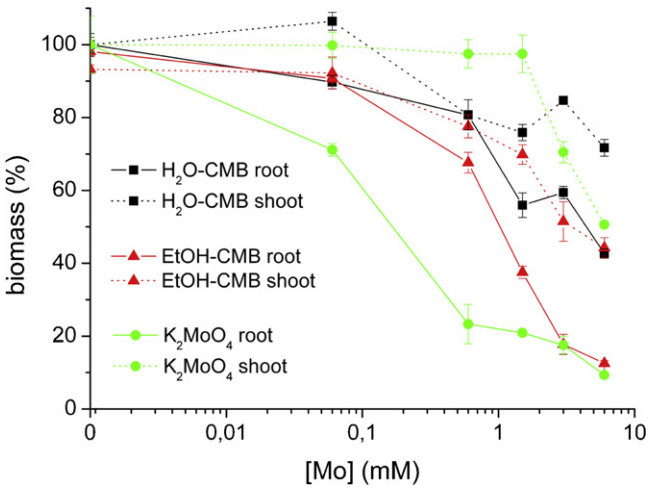

Fig. 3. Concentration–response curves for H_2O-CMB system (■), EtOH-CMB system (▲), and K_2MoO_4 solution (●). Results show separately root response (—) and shoot response (—). All the root and shoot growth data are respectively expressed as percentages of the root or shoot growth in H_2O negative control.

plants with either 2 mM CsBr, 14 mM KBr or 6 mM K_2MoO_4 water solutions, which simulate the maximum Cs, Br or Mo concentrations contained in a $Cs_2Mo_6Br_{14}$ solution at 1 mM. All the treatments with dissolved ions also affected the plants growth and here again roots were more affected than shoots ($p_{CsBr} = 1$ E−07, $p_{KBr} = 0.00007$, $p_{K_2MoO_4} = 0.0005$). The treatments with high concentrations of Cs^+ or Br^- ions resulted in a certain degree of growth inhibition, but their inhibitory effects, when existent, were always significantly lower than those of the clusters (Fig. 2). On the other hand, the treatment with K_2MoO_4 resulted in a very high growth inhibition, comparable or even higher than with EtOH-CMB system. Additional experiments have been performed using 2 mM CsBr, 14 mM KBr and 6 mM K_2MoO_4 mixed together in one single treatment, but the results did not show any synergic or additive effect and the growth inhibition was similar to K_2MoO_4 alone (data not shown).

In order to further characterize the growth inhibition capacity of the clusters and how this capacity is affected by the clusters state depending on the sorbing medium, concentration–response curves have been constructed (Fig. 3). Rapeseed plants have been treated with H_2O-CMB or EtOH-CMB with $Cs_2Mo_6Br_{14}$ concentrations of 0.01, 0.1, 0.25, 0.5 and 1 mM. These cluster concentrations correspond to Mo molar concentrations of 0.06, 0.6, 1.5, 3, and 6 mM respectively. Since we have seen that K_2MoO_4 treatments can cause similar or even higher growth inhibitions than cluster treatments, concentration–response curves have also been constructed for K_2MoO_4. Concentration–response curves showed that the effect of clusters on the plant growth was concentration dependent (Fig. 3). As already observed, the toxic effects were found in general more important for plants treated with ethanol-sorbed clusters than with water-sorbed clusters, and here again those effects were found more pronounced for roots (first significant effects at [Mo] = 0.06 mM, $p = 0.0100$) than for shoots (first significant effects at [Mo] = 0.6 mM, $p = 0.0102$). The concentration–response curves for the plants treated with K_2MoO_4 show different trends than for plants treated with clusters. For this treatment, the growth inhibition of the roots appears to evolve exponentially with the Mo concentration, whereas the shoots are not affected until a critical concentration (first significant effect at [Mo] = 3 mM).

3.3. *Effects of $Cs_2Mo_6Br_{14}$ on root morphology*

In addition to growth inhibition, it was visible from direct observation of the plants that clusters also had effects on the root morphology. Indeed, the plants treated with microsized (H_2O-CMB) clusters showed a high proliferation of root hairs, whereas the plants treated with nanosized (EtOH-CMB) clusters showed a perturbation of the root gravitropism (Supplementary information Fig. S5). In order to clarify those observations, the roots have been observed by FE-SEM (Fig. 4) for samples treated with 1 mM of clusters, and compared with negative control (H_2O). The plants treated with 6 mM of K_2MoO_4 have also been studied since the biomass results suggested similar effects as with ethanol-sorbed clusters at 1 mM (Fig. 2). It clearly appeared that the root tissues and root caps were much more affected and in a different manner when treated with EtOH-CMB compared to H_2O-CMB and even to K_2MoO_4 (Fig. 4). The control root and root cap look homogeneous and epidermal cells are visible, perfectly turgescent without any apparent damage. In contrast, for the plant treated with H_2O-CMB, the root shows the mentioned high root hairs proliferation, and the root cap looks eroded with the epidermal cells being hardly distinguishable. Concerning the root of a seedling treated with EtOH-CMB, it appears highly contorted, with an increased diameter, and the root tissues are fully eroded. The root cap also presents a completely different aspect, compared to control and to the root treated with H_2O-CMB, as it shows a smooth surface and is partially dissociated from the root. Finally, the root treated with K_2MoO_4 is homogeneous without apparent erosion, and with external root morphology being very similar to the control root in spite of the high growth inhibition induced by K_2MoO_4. This clearly suggests a different toxicological mechanism compared to cluster treatments.

3.4. *Uptake of $Cs_2Mo_6Br_{14}$ by rapeseed plants*

The interaction of microsized cluster aggregates with the vegetal tissues and their penetration into roots was first observed by FE-SEM on roots treated with H_2O-CMB (Supplementary information Fig. S6). These observations revealed an important concentration of cluster aggregates on the root surface. Moreover, some aggregates, hardly visible by FE-SEM in secondary electron detection (SE), appeared by backscattered electron detection (BSE) as shallowly embedded under the root surface. Some H_2O-CMB treated roots were broken few millimeters above the root apex after being

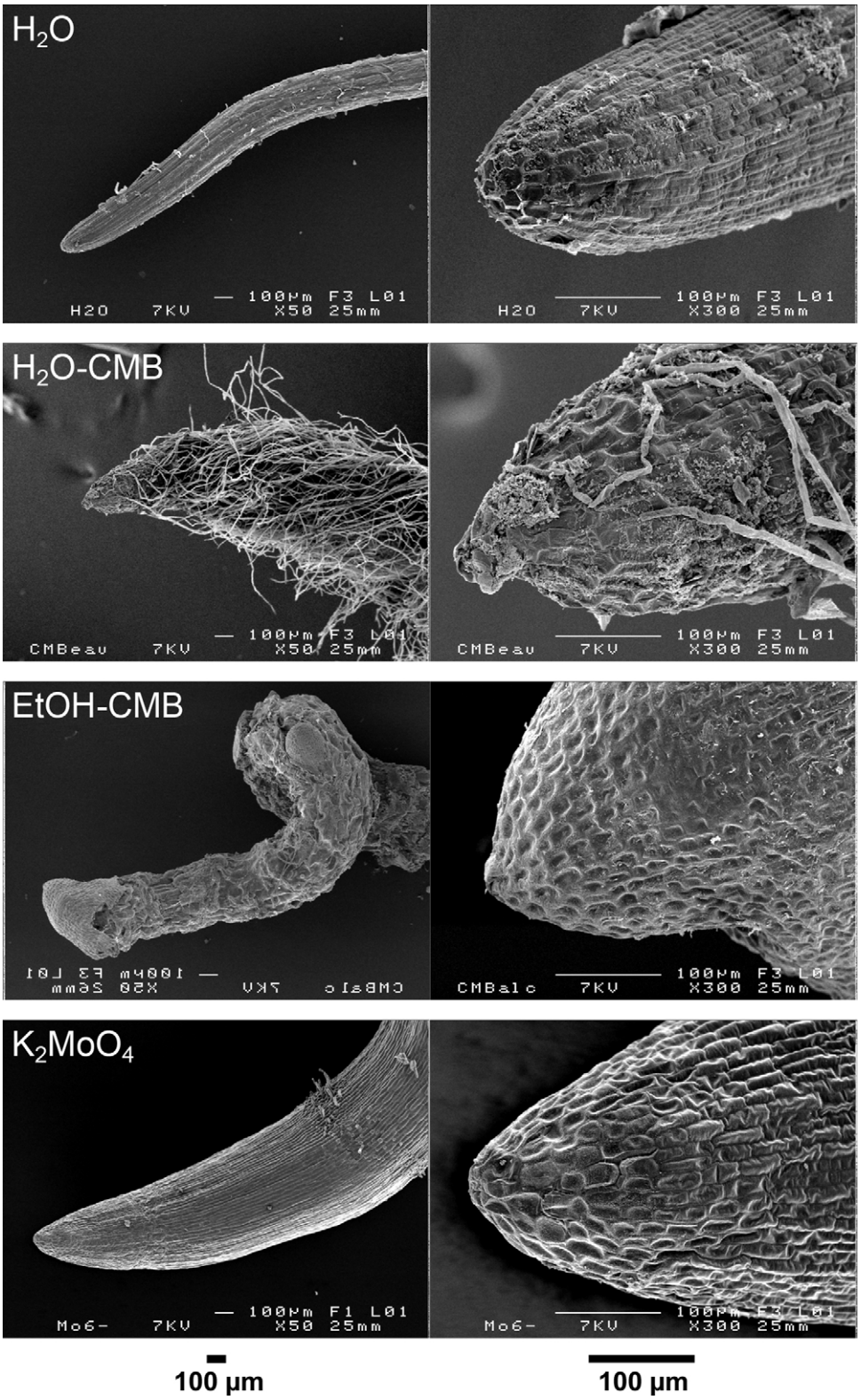

Fig. 4. FE-SEM images of roots after 5 days of growth in pure water (first row), 1 mM H_2O-CMB (second row), 1 mM EtOH-CMB (third row), and 6 mM K_2MoO_4 (fourth row).

completely dried by the CO_2 critical point method, and the inside of the root was observed again by FE-SEM (Supplementary information Fig. S7). Cluster aggregates were then also found inside the root and the comparison between SE and BSE images evidences that the cluster aggregates are intimately associated with the vegetal. They are slightly coated with organic matter, remarkable as it does not give a bright signal in BSE mode. In contrast, for plants treated with EtOH-CMB, it has never been possible to observe by FE-SEM the presence of clusters, neither on root surface nor inside the root (data not shown) although clusters aggregates were easily visible with the same technique on the substrate of this culture medium (Fig. 1).

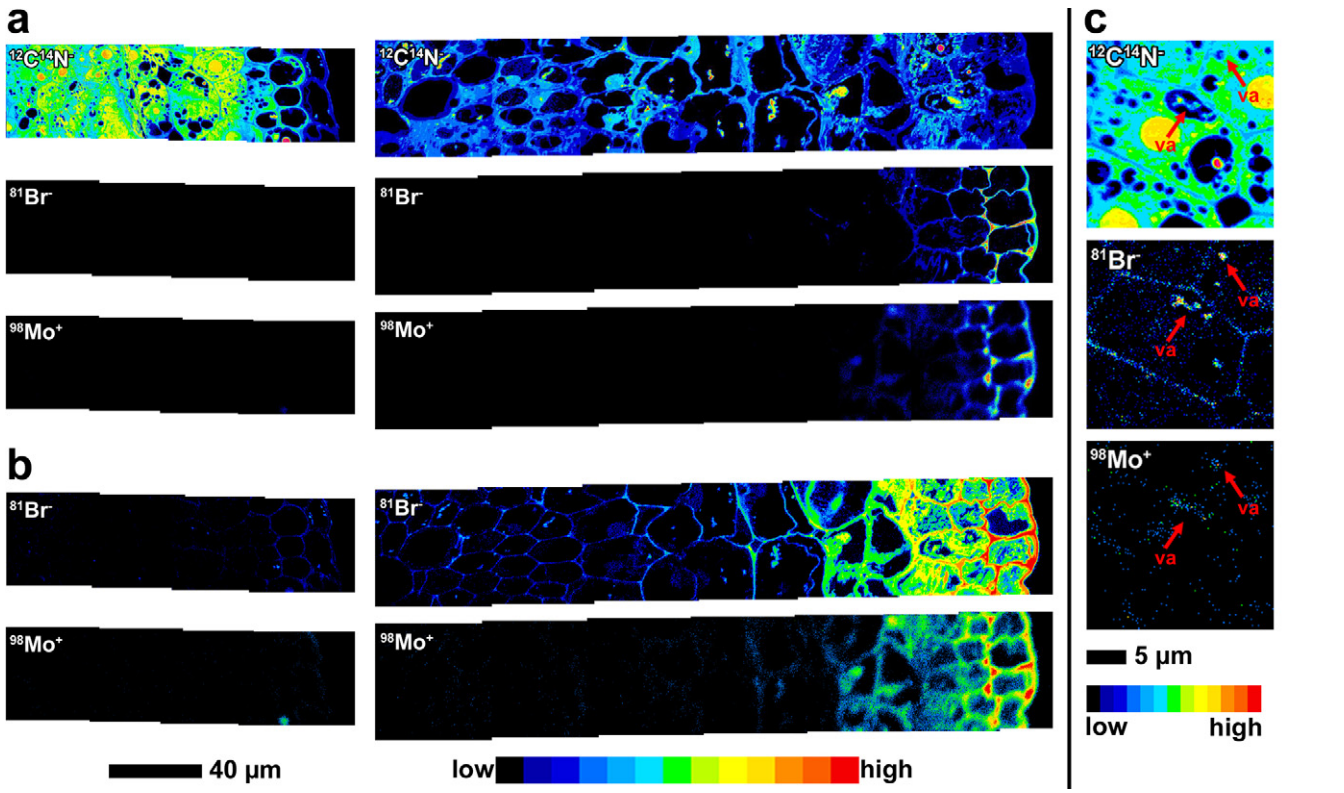

Fig. 5. NanoSIMS maps of $^{12}C^{14}N^-$, $^{81}Br^-$ and $^{98}Mo^+$ secondary ions in whole (a and b) or cortex (c) root cross sections of plants treated with a water-sorbing cluster suspension (left column in figures a and b, and figure c) or ethanol-sorbing cluster solution (right column in figures a and b), both at 1 mM, with (a and c) decimal and (b) logarithmic color scales. Analyzed samples are transversal sections of the roots, made few millimeters from the apex after chemical fixation, resin embedding and ultramicrotome sectioning. For every strip (a and b) the external part of the root is on the right side and the center of the root is on the left side of the strip. Arrows (c) indicate some cluster aggregates in vacuoles (va). (For interpretation of the references to color in this artwork, the reader is referred to the web version of the article.)

The clusters penetration was then carefully investigated by NanoSIMS, a high spatial resolution ion microprobe. This technique was found to be very powerful for such study as it allows the mapping of the elements of interest and to localize them in root cells thanks to the image of the vegetal matter which is obtained by the detection of the nitrogen atoms using $^{12}C^{14}N^-$ secondary ions. Thus, the clusters have been localized by mapping $^{81}Br^-$ and $^{98}Mo^+$ secondary ions in cross sections of the roots, few millimeters from the apex (see Supplementary information for details on the sample preparation). Fig. 5 shows an overview of the maps obtained for both culture systems. In these images, the signals can only be compared between treatments, but not between different elements as the intensity depend on the element sensibility to the ion beam (see Supplementary information). The $^{81}Br^-$ and $^{98}Mo^+$ maps evidenced that the clusters mainly penetrate in the root when it was treated with ethanol-sorbed clusters, whereas almost no clusters were observable in the root treated with water-sorbed clusters, considering decimal color scale (Fig. 5a). By applying a logarithmic function to the color scale, it was possible to visualize areas with low and high concentrations of clusters in the same image. Indeed, Fig. 5b displays the same $^{81}Br^-$ and $^{98}Mo^+$ maps with the colors in a logarithmic scale, and the EtOH-CMB $^{81}Br^-$ map nicely shows the distribution of clusters along the entire root cross section. Due to the lower sensitivity of the Mo element compared to Br for this technique, it was not possible to detect the low concentrations of Mo in the center part of the root, considering the acquisition parameters (see Supplementary information), but analysis with longer times of acquisition showed that Mo is sill present with the same distribution as Br in these areas (data not shown). The clusters were identified abundantly present in apoplast and symplast of the root epidermis, endodermis (cortex) and stele, with a concentration gradient decreasing from the epidermis to the stele. In addition, they do not appear as microsized aggregates but more as continuums. This suggests that mainly nanosized clusters can penetrate in the root and that this condition can only be achieved when clusters are dispersed in the culture medium with an ethanol-sorbing solution. However, confirming the FE-SEM observation of the inside of broken roots (Supplementary information Fig. S7), it was still possible to find few microsized cluster aggregates in roots treated with water-sorbing suspensions (Fig. 5c). Although the relative concentration of these aggregates is too low to be visible in Fig. 5a and b, they become visible in Fig. 5c thanks to a longer acquisition time (see Supplementary information), and are then found present in the vacuoles of the root.

4. Discussion

An appropriate characterization of nanomaterials is essential for toxicological evaluation as size, shape, aggregation, surface area or composition, among others, can potentially influence toxicity. Moreover, the properties of nanomaterials can change from the form in which they are synthesized to the form to which biological test systems are exposed. Consequently, in addition to the characterization of synthesized nanosized $Cs_2Mo_6Br_{14}$ clusters, we tried here to analyze clusters in the vehicle in which it is administered, in the test system and finally within the biological system. Even if cluster units are nanosized entities, they are hydrolyzed in presence of water and co-precipitate with water molecules to form the crystalline compound $[(Mo_6Br^i_8)(OH)^a_4(H_2O)^a_2]\cdot 12H_2O$ that adopts the shape of disc-like aggregates (up to few micrometers) in water. However, the clusters formed smaller aggregates

(up to several hundred nanometers) when they were introduced on the culture substrate in a nanosized form (EtOH-CMB). Thus, in our systems, the interactions of the clusters with the paper seem to protect them to some extent from aggregation. This is in agreement with previous studies already showing that the interaction of nanoparticles with organic matter can reduce particle aggregation [20,21]. It was even found that in the EtOH-CMB system, at least 21% of the clusters remained in the liquid medium as nanosized entities.

Toxicity tests showed that all the treatments with clusters resulted in a concentration-dependent inhibition of the rapeseed growth, with the roots being more affected than the shoots. However, treatments with microsized cluster aggregates (H_2O-CMB) resulted in limited toxic effects compared to treatments with nanosized clusters (EtOH-CMB) which resulted in a high growth inhibition (up to 86% for treatments with 1 mM $Cs_2Mo_6Br_{14}$). The differences in growth inhibitions for the same initial mass of cluster compound indicate that the concentration-dependent toxicity of the Mo_6 clusters depend on their aggregation state. Indeed, we have shown that the clusters and cluster aggregates can be found in a wide range of sizes depending on the dispersing medium, with specific surfaces areas that can theoretically vary between 7 and 1000 m^2/g.

The toxic effects of metal-based nanoparticles can be incremented by the release of metal ions or other components in the dissolution process. From literature and our own analysis (Figs. 2 and 3), the most toxic component of clusters is molybdenum, an essential micronutrient but also a heavy metal which is toxic at high concentrations [22]. Even if plants are fairly tolerant to Mo, excessive Mo application can impair nitrogen metabolism and thus reduce normal plant growth [22]. We have shown by ICP-OES and XPS analysis that cluster hydrolysis happened in our culture medium (Supplementary information Fig. S4) but it only concerned the apical Br ligands and the Cs counter cations, and no Mo was released in the solution as ionic species. Concerning Cs^+ and Br^- ions, the phytotoxicity tests showed that both ions induced some growth inhibitions in good agreement with previous studies [23,24], but it did not reach the high growth inhibition found in the case of treatments with ethanol-sorbed clusters (Fig. 2). Finally, the possible influence of an acidic pH resulting from the cluster hydrolysis is hardly discussable because rapeseed plants were able to neutralize the pH of the medium (Supplementary information Fig. S2). In addition, pH effects could not explain the important differences existing between the H_2O-CMB and EtOH-CMB systems as we did not observe pH differences between both mediums.

Concerning the interactions of the cluster aggregates with the plant root surface, they were found to be adsorbed in close contact with root tissues (Supplementary information Fig. S6). From the FE-SEM images of the external part of the roots (Fig. 4), it was clear that the clusters severely damaged the epidermal cells and even the cortical cells in the case of EtOH-CMB. In addition to root growth inhibition, differences in root morphology were observed depending on the size of the cluster aggregates. Thus, while microsized cluster aggregates enhanced hypertrophied root hair production even at proximity of the root cap, nanosized clusters treatment resulted in stunted plants, and a loss of gravitropism. This agravitropism must be due to the observed highly deteriorated root cap as it is where the primary site for gravity sensing is located [25]. Provided that MoO_4^{2-} affected root morphology in a different way than the clusters (Fig. 4), and that the Mo from the clusters is not liberated, we can conclude that the phytotoxicity of the clusters must result from particular physical and chemical interactions with root growth.

Histological examination of the tissues exposed to nanomaterials is determinant to characterize their distribution and effects. Here, the NanoSIMS technique provided very useful information on the uptake of clusters. Other techniques have already been used to localize elements or even nanoparticles in plants, such as SEM coupled with energy dispersion spectroscopy [26], transmission electron microscopy [14,15,27,28], confocal microscopy [14,28], two-photon excitation microscopy [29], or micro X-ray fluorescence using a synchrotron radiation and combined with X-ray absorption near edge structure spectroscopy [26], but these techniques have shown some limits and prospecting for new monitoring possibilities remains an important task. In this frame, the NanoSIMS technique was found to be a very powerful technique for studying the root uptake and localization of elements inside the plant with a high spatial resolution, and which could be applied to a wide range of elements. Indeed, here NanoSIMS results showed that cluster penetration in the root was much more important in the ethanol-sorbing system (Fig. 5). As suggested by ICP-OES analyses and UV absorption of the liquid medium, in the EtOH-CMB system an important part of the clusters remains as nanosized entities which therefore easily penetrate and translocate into the root, provoking a high growth inhibition and important damages to the root morphology. In addition, NanoSIMS allowed observing a gradient of concentration in the root cross section. Clusters were observed at higher concentrations in the apoplast of the epidermal and cortical cells, pleading for an apoplastic penetration pathway through the root epidermis and cortex. The clusters were also observed inside the cells and in some cases microsized aggregates showed to be accumulated inside vacuoles (Fig. 5c), but it is unclear whether they were transported there as nanosized individuals or as aggregates. The vacuole sequestration of nanoparticles in plant cells has also been reported by Etxeberria et al. [30]. However, in spite of the capacity to penetrate cells and thus the intrinsic possibility to pass to the stele avoiding the endodermal casparian strip, no cluster was observed inside vascular cells. In most described cases of nanoparticles uptake by plants, the substantial longitudinal movement of nanoparticles in plants, either from root to shoot via xylem or from source to sink organs via phloem, showed to be very limited with short distance movements been favored [15,27–29,31].

In summary, hexamolybdenum clusters provided by $Cs_2Mo_6Br_{14}$ were found to have important toxic effects on rapeseed plants. Although the consequences of the partial cluster hydrolysis, i.e. release of dissolved Cs^+ and Br^- ions, were found to contribute to the overall toxicity, the importance of the size of the cluster aggregates has also been evidenced and showed to be preponderant. Indeed, treatments with microsized cluster aggregates resulted in limited toxic effects, whereas treatments with nanosized clusters resulted in a higher growth inhibition and in important damages on the root morphology, likely due to an easier penetration of the clusters in the root as evidenced by NanoSIMS analysis. The high specific surface area of these nanosized clusters induces then high toxic effects. As a matter of fact, for applications in biotechnologies the doses of nanoparticles are far below those tested in this work [32]. However, the lowest concentration of clusters used here (10 μM) already showed significant toxic effects on growth. Considering that rapeseed is not a very sensitive plant species and that we did not test chronic exposure, one can expect the no-observed-effect concentration for $Cs_2Mo_6Br_{14}$ will be considerably lower than 10 μM. As a consequence, such material should be handled with care since it can have harmful effects on organisms. Hence, for biotechnological applications these clusters should be embedded in a biocompatible matrix such as silica. The embedding of $Cs_2Mo_6Br_{14}$ in silica nanoparticles has been the subject of already published works [6–8]; the evaluation of the toxicity of those cluster@SiO_2 nanoparticles is now under progress, and so far no toxic effect has been found.

Acknowledgements

This work was supported by the ANR (2011 BS0801301), University of Rennes 1, CNRS, Région Bretagne. The authors thank J. Le Lannic (CMEBA) for supplying the FE-SEM images, M.-T. Lavault and V. Gouesbet for the ultrathin sections mounted for NanoSIMS, T. Delhaye (platform ONIS/EuropIA with funds from FEDER, Région Bretagne and Rennes Métropole) for the NanoSIMS analysis, S. Ababou-Girard and C. Meriadec for the XPS analyses, and Y. Le Gal for the ICP-OES analyses.

Appendix A. Supplementary data

Supplementary data associated with this article can be found, in the online version, at http://dx.doi.org/10.1016/j.jhazmat.2012.03.058.

References

[1] C. Buzea, I.I. Pacheco, K. Robbie, Nanomaterials and nanoparticles: sources and toxicity, Biointerphases 2 (2007) MR17–MR71.
[2] W.-X. Zhang, B. Karn, Nanoscale environmental science and technology: challenges and opportunities, Environ. Sci. Technol. 39 (2005) 94A–95A.
[3] E. Roduner, Size matters: why nanomaterials are different, Chem. Soc. Rev. 35 (2006) 583–592.
[4] T. Xia, N. Li, A.E. Nel, Potential health impact of nanoparticles, Annu. Rev. Public Health 30 (2009) 137–150.
[5] M.N. Rhyner, A.M. Smith, X. Gao, H. Mao, L. Yang, S. Nie, Quantum dots and multifunctional nanoparticles: new contrast agents for tumor imaging, Nanomedicine 1 (2006) 209–217.
[6] F. Grasset, F. Dorson, S. Cordier, Y. Molard, C. Perrin, A.M. Marie, T. Sasaki, H. Haneda, Y. Bando, M. Mortier, Water-in-oil microemulsion preparation and characterization of $Cs_2Mo_6X_{14}$@SiO_2 phosphor nanoparticles based on transition metal clusters (X = Cl, Br, and I), Adv. Mater. 20 (2008) 143–148.
[7] F. Grasset, F. Dorson, Y. Molard, S. Cordier, V. Demange, C. Perrin, V. Marchi-Artzner, H. Haneda, One-pot synthesis and characterizations of bi-functional phosphor-magnetic @SiO_2 nanoparticles: controlled and structured association of Mo_6 cluster units and γ-Fe_2O_3 nanocrystals, Chem. Commun. (2008) 4729–4731.
[8] T. Aubert, F. Grasset, S. Mornet, E. Duguet, O. Cador, S. Cordier, Y. Molard, V. Demange, M. Mortier, H. Haneda, Functional silica nanoparticles synthesized by water-in-oil microemulsion processes, J. Colloid Interface Sci. 341 (2010) 201–208.
[9] J.R. Long, X. Xheng, R.H. Holm, S.-B. Yu, M. Droege, W.A. Sanderson, Contrast agents, U.S. Patent 5,804,161 (1998).
[10] G.L. Baker, R.N. Ghosh, D.J. Osborn Iii, Sol–gel encapsulated hexanuclear clusters for oxygen sensing by optical techniques, U.S. Patent 7,858,380 (2010).
[11] Y. Molard, S. Cordier, M. Amela-Cortes, F. Dorson, Luminescent hybrid liquid crystal, U.S. Patent 2011/0130565 (2011).
[12] A. Ostrowski, T. Martin, J. Conti, I. Hurt, B. Harthorn, Nanotoxicology: characterizing the scientific literature, 2000–2007, J. Nanopart. Res. 11 (2009) 251–257.
[13] EPA 712-C-96-154, Ecological Effects Test Guidelines (OPPTS 850.4200): Seed Germination/Root Elongation Toxicity Test, United States Environmental Protection Agency, Washington, DC, 1996, www.epa.gov/opptsfrs/publications/OPPTS_Harmonized/850_Ecological_Effects_Test_Guidelines/Drafts/850-4200.pdf.
[14] X. Ma, J. Geiser-Lee, Y. Deng, A. Kolmakov, Interactions between engineered nanoparticles (ENPs) and plants: phytotoxicity, uptake and accumulation, Sci. Total Environ. 408 (2010) 3053–3061.
[15] E. Corredor, P. Testillano, M.-J. Coronado, P. González-Melendi, R. Fernandez-Pacheco, C. Marquina, M.R. Ibarra, J. de la Fuente, D. Rubiales, A. Perez-de-Luque, M.-C. Risueno, Nanoparticle penetration and transport in living pumpkin plants: in situ subcellular identification, BMC Plant Biol. 9 (2009) 45.
[16] N.C. Carpita, D.M. Gibeaut, Structural models of primary cell walls in flowering plants: consistency of molecular structure with the physical properties of the walls during growth, Plant J. 3 (1993) 1–30.
[17] C.M. Rico, S. Majumdar, M. Duarte-Gardea, J.R. Peralta-Videa, J.L. Gardea-Torresdey, Interaction of nanoparticles with edible plants and their possible implications in the food chain, J. Agric. Food. Chem. 59 (2011) 3485–3498.
[18] S. Cordier, K. Kirakci, D. Méry, C. Perrin, D. Astruc, Nanocluster cores (X = Br, I): from inorganic solid state compounds to hybrids, Inorg. Chim. Acta 359 (2006) 1705–1709.
[19] J.C. Sheldon, Bromo- and iodo-molybdenum(II) compounds, J. Chem. Soc. (1962) 410–414.
[20] H. Hyung, J.D. Fortner, J.B. Hughes, J.-H. Kim, Natural organic matter stabilizes carbon nanotubes in the aqueous phase, Environ. Sci. Technol. 41 (2007) 179–184.
[21] A.A. Keller, H. Wang, D. Zhou, H.S. Lenihan, G. Cherr, B.J. Cardinale, R. Miller, Z. Ji, Stability and aggregation of metal oxide nanoparticles in natural aqueous matrices, Environ. Sci. Technol. 44 (2010) 1962–1967.
[22] C. Baldisserotto, L. Ferroni, C. Zanzi, R. Marchesini, A. Pagnoni, S. Pancaldi, Morpho-physiological and biochemical responses in the floating lamina of *Trapa natans* exposed to molybdenum, Protoplasma 240 (2010) 83–97.
[23] R.S. Bowman, J. Schroeder, R. Bulusu, M. Remmenga, R. Heightman, Plant toxicity and plant uptake of fluorobenzoate and bromide water tracers, J. Environ. Qual. 26 (1997) 1292–1299.
[24] Y. Su, B. Maruthi Sridhar, F. Han, S. Diehl, D. Monts, Effect of bioaccumulation of Cs and Sr natural isotopes on foliar structure and plant spectral reflectance of Indian mustard (*Brassica Juncea*), Water Air Soil Pollut. 180 (2007) 65–74.
[25] M.T. Morita, Directional gravity sensing in gravitropism, Annu. Rev. Plant Biol. 61 (2010) 705–720.
[26] M.-P. Isaure, B. Fayard, G. Sarret, S. Pairis, J. Bourguignon, Localization and chemical forms of cadmium in plant samples by combining analytical electron microscopy and X-ray spectromicroscopy, Spectrochim. Acta B 61 (2006) 1242–1252.
[27] D. Lin, B. Xing, Root uptake and phytotoxicity of ZnO nanoparticles, Environ. Sci. Technol. 42 (2008) 5580–5585.
[28] P. González-Melendi, R. Fernandez-Pacheco, M.J. Coronado, E. Corredor, P.S. Testillano, M.C. Risueno, C. Marquina, M.R. Ibarra, D. Rubiales, A. Perez-de-Luque, Nanoparticles as smart treatment-delivery systems in plants: assessment of different techniques of microscopy for their visualization in plant tissues, Ann. Bot. 101 (2008) 187–195.
[29] E. Wild, K.C. Jones, Novel method for the direct visualization of in vivo nanomaterials and chemical interactions in plants, Environ. Sci. Technol. 43 (2009) 5290–5294.
[30] E. Etxeberria, P. Gonzalez, E. Baroja-Fernandez, J. Pozueta Romero, Fluid phase endocytic uptake of artificial nano-spheres and fluorescent quantum dots by sycamore cultured cells: evidence for the distribution of solutes to different intracellular compartments, Plant Signal. Behav. 1 (2006) 196–200.
[31] H. Zhu, J. Han, J.Q. Xiao, Y. Jin, Uptake, translocation, and accumulation of manufactured iron oxide nanoparticles by pumpkin plants, J. Environ. Monit. 10 (2008) 713–717.
[32] A.A. Burns, J. Vider, H. Ow, E. Herz, O. Penate-Medina, M. Baumgart, S.M. Larson, U. Wiesner, M. Bradbury, Fluorescent silica nanoparticles with efficient urinary excretion for nanomedicine, Nano Lett. 9 (2009) 442–448.